EJN fens European Journal of Neuroscience

European Journal of Neuroscience, Vol. 30, pp. 1092–1100, 2009 doi:10.1111/j.1460-9568.2009.06883.x

NEUROSYSTEMS

Inbred mouse strains differ in multiple hippocampal activity traits

R. Jansen,[1] K. Linkenkaer-Hansen,[2] T. Heistek,[2] J. Timmerman,[2] Huibert D. Mansvelder,[2] Arjen B. Brussaard,[2] M. de Gunst[1] and A. van Ooyen[2]

[1]Department of Mathematics, VU University Amsterdam, Amsterdam, The Netherlands

[2]Department of Integrative Neurophysiology, Center for Neurogenomics and Cognitive Research, Neuroscience Campus Amsterdam, VU University Amsterdam, De Boelelaan 1085, 1081 HV Amsterdam, The Netherlands

Keywords: gamma oscillations, genetic correlation, heritability, hippocampus

Abstract

A major challenge in neuroscience is to identify genes that influence specific behaviors and to understand the intermediary neuronal mechanisms. One approach is to identify so-called endophenotypes at different levels of neuronal organization from synapse to brain activity. An endophenotype is a quantitative trait that is closer to the gene action than behavior, and potentially a marker of neuronal mechanisms underlying behavior. Hippocampal activity and, in particular, hippocampal oscillations have been suggested to underlie various cognitive and motor functions. To identify quantitative traits that are potentially useful for identifying genes influencing hippocampal activity, we measured gamma oscillations and spontaneous activity in acute hippocampal slices from eight inbred mouse strains under three experimental conditions. We estimated the heritability of more than 200 quantitative traits derived from this activity. We observed significant differences between the different mouse strains, particularly in the amplitude of the activity and the correlation between activities in different hippocampal subregions. Interestingly, these traits had a low genetic correlation between the three experimental conditions, which suggests that different genetic components influence the activity in different conditions. Our findings show that several traits of hippocampal gamma oscillations and spontaneous activity are heritable and could thus be potentially useful in gene-finding strategies based on endophenotypes.

Introduction

Several studies have shown that numerous aspects of cognition are substantially influenced by genetic factors (Plomin & Crabbe, 2000). These genetic factors can shed light on the physiological processes involved in cognition. Therefore, it is important to identify genes that code for complex cognitive traits. Progress in this field remains limited, however, because of the presumably large number of genes involved (de Geus, 2002). One way to overcome this problem is to identify genes that shape the physiological processes underlying the complex traits. It is assumed that quantitative markers of these processes – also known as endophenotypes – are governed by only a subset of the genes influencing the behavioral trait (Gottesman & Gould, 2003; Flint & Munafo, 2007). Several definitions of an endophenotype have been proposed, but they all have in common that in order for a trait to be classified as an endophenotype, it has to be heritable and co-segregated with a brain disease or a cognitive trait.

The hippocampus plays an important role in the formation of episodic memories (Cohen & Eichenbaum, 1993; Squire & Butters, 2002). In memory tasks, the power of hippocampal gamma oscillations and the coherence between the hippocampal subregions CA3 and CA1 have been shown to increase in rodents (Montgomery & Buzsáki, 2007). Similar oscillations can be pharmacologically induced in hippocampal slices of rodents with the cholinergic agonist carbachol, which mimics the cholinergic input that comes from the brainstem in intact brains (Shute & Lewis, 1963; Fisahn *et al.*, 1998; Mann *et al.*, 2005). These oscillations originate in the CA3 region and depend on muscarinic acetylcholine receptor activation and perisomatic inhibition (Fisahn *et al.*, 1998; Mann *et al.*, 2005). The *in vitro* oscillations are comparable to *in vivo* gamma oscillations, as they both arise from CA3 and have similar sink-source distributions (Csicsvari *et al.*, 2003). This suggests that key physiological mechanisms of, for instance, spatial memory may be studied *in vitro*. Using this paradigm, as a first step towards the identification of endophenotypes for memory-related behavior or diseases, we recorded hippocampal spontaneous activity and carbachol-induced oscillations with multi-electrode arrays in a number of inbred mouse strains.

Zolpidem is a non-benzodiazepine $GABA_A$ receptor modulator that increases inhibition during carbachol-induced gamma oscillations (Hájos *et al.*, 2000; Pálhalmi *et al.*, 2004). To investigate the differences across mouse strains with respect to the involvement of GABAergic transmission in oscillations, we also studied the effects of zolpidem on gamma oscillations.

The primary traits that are generally investigated in studies on the functions and mechanisms of neuronal network oscillations are ampli-

Correspondence: Dr A. van Ooyen, as above.
E-mail: arjen.van.ooyen@cncr.vu.nl

Received 9 April 2009, revised 3 July 2009, accepted 6 July 2009

tude and interactions between brain areas. Therefore, we focused on investigating the heritability of these traits in the mouse hippocampus.

Materials and methods

Slice preparation and recording

All experiments were performed in accordance with the guidelines and with the approval of the Animal Welfare Committee of the VU University Amsterdam, which operates in accordance with Dutch and European law. The eight inbred mouse strains (129S1SvImJ, A/J, Balb/cByJ, C3H/HeJ, C57Bl6/J, DBA/2J, FVB/NJ, and NOD/LtJ; see Fig. 1A) were obtained from Jackson Laboratories. These strains are known to differ in many behavioral and physical phenotypes, and are currently also analysed in the Mouse Phenome Database (http://www.jax.org/phenome), where they form a proportion of the top-priority mouse strains, owing to their widespread usage and genetic diversity (Fernandes *et al.*, 2004; Hovatta *et al.*, 2005). Non-anesthetized mice were decapitated at postnatal day 13–15. Animals of this age were used because more cells die in slices of older animals, which makes it more difficult to induce oscillations. The brains were quickly removed and placed in ice-cold artificial cerebrospinal fluid (ACSF) containing 125 mM NaCl, 25 mM $NaHCO_3$, 3 mM KCl, 1.2 mM NaH_2PO_4, 1 mM $CaCl_2$, 3 mM $MgSO_4$, and 10 mM D-glucose (carboxygenated with 5% CO_2/95% O_2). Horizontal slices (400 μm thick) from the ventral hippocampus were cut with a microtome (Microm, Waldorf, Germany). Slices were stored in an interface storage chamber at room temperature, and placed in ACSF containing 2 mM $CaCl_2$ and 2 mM $MgSO_4$. After 1 h, slices were placed on eight-by-eight planar electrode grids with 200 μm spacing between the

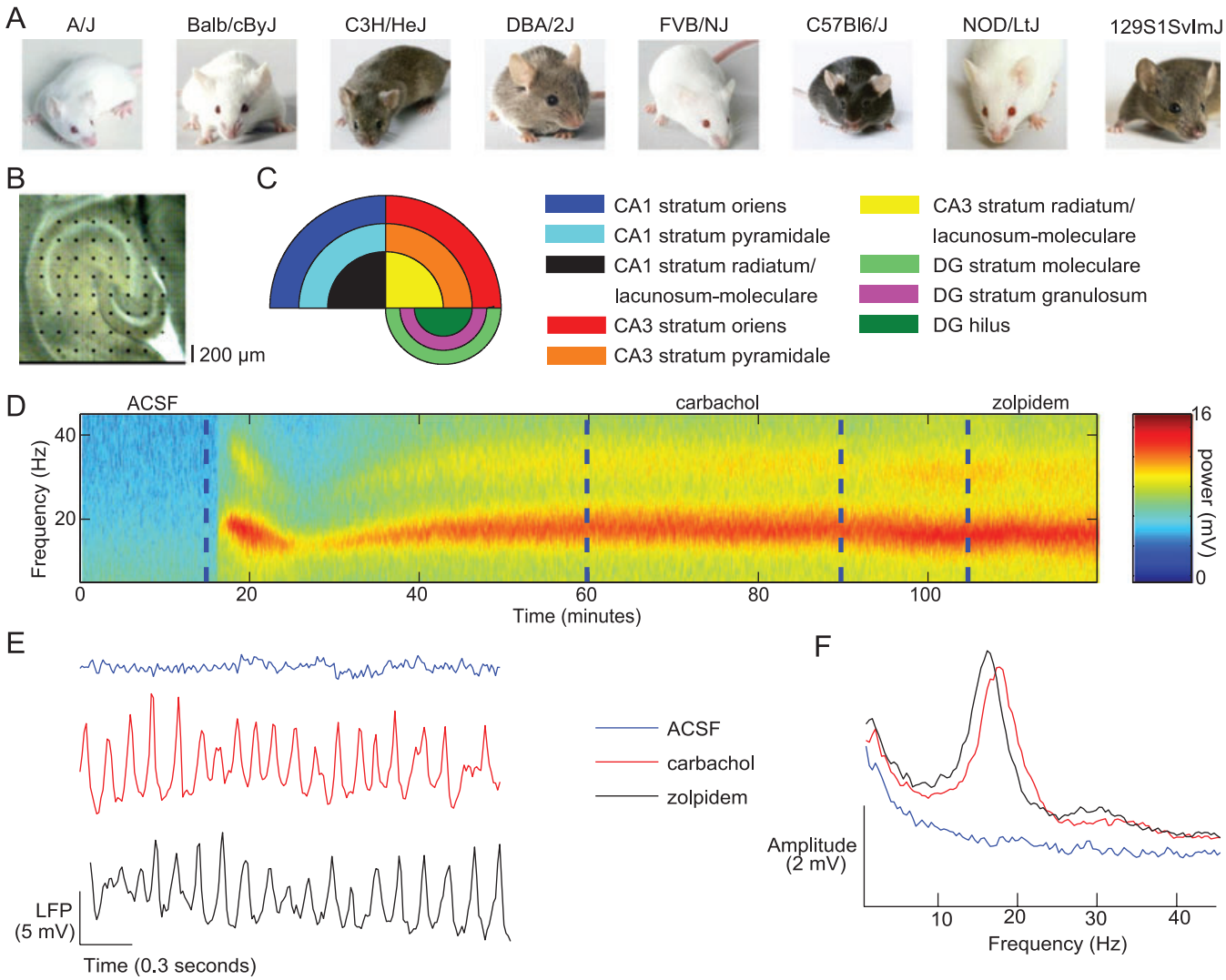

FIG. 1. Fourier analysis of hippocampal local field potentials measured from eight inbred mouse strains in three experimental conditions. (A) Typical appearances of the eight mouse strains (reproduced with permission from The Jackson Laboratory). (B) A multi-electrode array covering a slice of the hippocampus. Black dots are electrodes that are separated by 200 μm. For every slice, a photograph was taken to classify the electrodes into the nine hippocampal subregions shown in C. (D) Time–frequency representation of a signal in the stratum oriens in CA3 for the complete experimental protocol. (E) Examples of local field potential (LFP) broadband traces (0–100 Hz) in the artificial cerebrospinal fluid (ACSF) (blue), carbachol (red) and zolpidem (black) conditions. (F) Amplitude spectra of representative signals in each condition. The traits that were derived from these curves are the integrated amplitudes in the frequency intervals 1–4, 4–7, 7–13, 13–25, 25–35 and 35–45 Hz. From the spectra obtained in the carbachol and zolpidem conditions, we also derived peak amplitudes. Note that the frequencies of the oscillations fall below the gamma range at low bath temperatures in the recording units.

60 electrodes (the four corners of the grid did not contain electrodes; see Fig. 1B) and polyethylenimine coating (Sigma, St Louis, MO, USA). The slices were left for 1 h in a chamber with humidified carbogen gas before they were placed in the recording unit. During recordings, the flow rate was 4–5 mL/min and the temperature was kept at 30 ± 0.3°C. Zolpidem was purchased from Duchefa (Haarlem, The Netherlands) and dissolved in dimethylsulfoxide (0.00001%): carbachol was purchased from Sigma. Local field potentials were sampled at 1 kHz and down-sampled off-line to 200 Hz and converted into MATLAB (The Mathworks, Natick, MA, USA) file format. Off-line analysis was done using custom written scripts in MATLAB.

Experimental protocol

During each recording session, four slices (obtained from two different animals) were recorded simultaneously, in four identical recording units. After the slices had been placed in the recording units with ACSF, 15 min of spontaneous activity was recorded (Fig. 1D). These first 15 min will be referred to as the 'ACSF condition'. Carbachol (25 μM) was then bath applied to the slice. Carbachol-induced oscillations were initially unstable in frequency and amplitude, but stabilized after 45 min. After this 45 min wash-in period, gamma oscillations were recorded for a period of 30 min, which will be referred to as the 'carbachol condition'. Subsequently, zolpidem (100 nM) and carbachol (25 μM) were washed in for 30 min, the last 15 min of which were used to analyse oscillations. This period will be referred to as the 'zolpidem condition'. In Fig. 1D, a time–frequency representation of a representative signal is shown for the complete experimental procedure. Examples of local field potential traces for each condition separately are shown in Fig. 1E.

Slice selection and pre-analysis

For each experiment, a photograph was taken of the slices in the recording unit, in order to visualize the locations of the electrodes in the hippocampus (Fig. 1B). The hippocampus consists of three main anatomical regions: CA1, CA3, and the dentate gyrus (DG). CA3 and CA1 were divided into the subregions stratum oriens, stratum pyramidale, and stratum radiatum/lacunosum-moleculare, and the DG into the stratum moleculare, stratum granulosum, and hilus (Fig. 1C). To classify an electrode as lying in one of these nine hippocampal subregions, an interactive MATLAB procedure (written in-house) based on the photograph of the electrode grid, was used. Using Fourier analysis (see below), whether oscillatory activity was present was determined for each channel. If none of the 60 channels showed oscillations, the slice was excluded from further analysis. In total, 120 slices were analysed (distribution over strains: A/J, n = 22; Balb/cByJ, n = 10; C3H/HeJ, n = 14; DBA/2J, n = 18; FVB/NJ, n = 20; C57Bl6/J, n = 12; NOD/LtJ, n = 14; 129S1SvImJ, n = 10).

In order to reject artifacts before the quantitative trait analysis, each slice recording was subjected to a principle component analysis. This resulted in 64 eight-by-eight spatial components, with corresponding temporal principal component scores. If noisy channels were present, then the first few spatial components had high values only for one or a few of these channels. These channels were identified and excluded. The time series of the remaining channels were averaged and plotted to identify and exclude noisy intervals.

Fourier analysis

For all three conditions (ACSF, carbachol, and zolpidem), and for each electrode that was classified into one of the nine regions, the Fourier amplitude spectrum was calculated using Welch's method (Welch, 1967). See Fig. 1F for representative spectra in the three conditions. From these spectra, the integrated amplitude in the frequency bands 1–4, 4–7, 7–13, 13–25, 25–35 and 35–45 Hz was calculated. For the carbachol and zolpidem conditions, the peak amplitude was also calculated. For each of these measures, the traits analysed were the means per region. To establish whether oscillations were detected at a given electrode, the following procedure was applied. First, a frequency interval in which the peak of the spectrum occurred was determined visually; for example, for the spectrum in Fig. 1F, this interval would be from 10 to 25 Hz. Next, a $1/f$ curve was fitted to the spectrum outside this interval. This $1/f$ curve was then subtracted from the original spectrum. Finally, a Gaussian curve was fitted to the remaining spectrum. If the peak of this Gaussian curve did not exceed the 95% confidence interval of the fitted $1/f$ curve, the signal was classified as not oscillating. Slices were excluded from further analysis when none of the channels detected oscillations.

Interaction between hippocampal regions

To quantify the interaction between two different hippocampal regions, for example between the CA1 stratum oriens and the CA3 stratum oriens, a suitable measure was calculated (as described below) between all possible pairs of channels from these regions, from which the mean was then taken. This was done for all region pairs. Before this analysis, the signals were filtered between 5 and 40 Hz to remove the fairly large amount of noise outside this interval.

Oscillatory activity was not observed in the ACSF condition, and therefore channel interactions in this condition were quantified using (Pearson linear) correlation of the local field potentials. Thus, for every pair of regions, and for all possible electrode pairs between these regions, the correlation of the local field potentials at these electrodes was computed, and the mean of these correlations was used in further analysis. In the carbachol and zolpidem conditions, in contrast, the signals were strongly oscillatory. Therefore, the phase-locking factor (PLF) between channels was calculated in these conditions. The PLF is a well-established measure for quantifying the interaction between two oscillating signals that can be out of phase and possibly have independent amplitude fluctuations (Tass *et al.*, 1998; Lachaux *et al.*, 1999).

To obtain a better estimate of the location of oscillatory activity than can be provided by multi-electrode measurements of local field potentials, the current-source density of the local field potentials was computed (Mitzdorf, 1985; Mann *et al.*, 2005). After this transformation, the PLF between channels was again computed. The results obtained from the PLFs of the raw data and those from the current-source density-transformed data were similar. Because the latter showed more significant differences between strains, only these are reported.

Normalization

For specific analysis of the effect of carbachol, the trait values of carbachol-induced oscillations were normalized by dividing them by the trait values from the ACSF condition. As not all of the traits were present in both conditions, the peak power from the carbachol condition was divided by the integrated amplitude between 15 and 25 Hz from the ACSF condition. The PLF traits from the carbachol condition were divided by the correlation traits from the ACSF condition. Similarly, for analysis of the effect of zolpidem, the zolpidem-trait values were divided by the carbachol-trait values. Thus,

the normalized traits express the relative sensitivity to experimental manipulations. Subtractive normalization instead of divisive normalization yielded similar results.

ANOVA

To determine whether a trait differs significantly between mouse strains, a one-way ANOVA with the trait as dependent variable and mouse strain as factor, and the corresponding F-test, were performed for every trait. The null hypothesis of this test is that for at least one strain the trait mean, that is, the expected value, is significantly different from the trait means of the other strains. Where necessary, the data were log-transformed in order not to violate the normality assumption for ANOVA.

Heritability

The observed value of a trait from a single slice and a single animal is the result of both genetic and environmental influences. To investigate the extent to which a trait is influenced by genetic factors, we may estimate its heritability. The heritability of a trait is a measure of the proportion of the total variance of the trait that is caused by genetic variation. The remainder of the variance is assumed to be due to environmental factors. To define the heritability of a trait and to illustrate how it is estimated, let X_{ij} denote the jth observation ($j = 1, \ldots, n_i$) of the ith strain for the trait ($i = 1, \ldots, I$) and let.

$$N = \sum_{i=1}^{I} n_i$$

be the total number of observations of the trait. Furthermore, let

$$X_i = \frac{1}{n_i} \sum_{j=1}^{n_i} X_{ij}$$

denote the mean of the observations for the ith strain, and

$$X = \frac{1}{N} \sum_{i=1}^{I} \sum_{j=1}^{n_i} X_{ij}$$

the mean of all observations. For inbred strains, the heritability h^2 of a trait can be defined as

$$h^2 = \frac{\sigma_G^2/2}{\sigma_G^2/2 + \sigma_E^2}$$

where $\sigma^2{}_G$ is the component of variance between strains, and $\sigma^2{}_E$ is the component of variance within strains (Hegmann & Possidente, 1981). The value of h^2 ranges between 0 and 1, where 0 means no genetic contribution to the trait, and 1 means that the trait is controlled only by genetic factors. The heritability h^2 can be estimated as

$$\hat{h}^2 = \frac{(MS_{\text{between}} - MS_{\text{within}})/(2n^*)}{(MS_{\text{between}} - MS_{\text{within}})/(2n^*) + MS_{\text{within}}}$$

where

$$MS_{\text{within}} = \frac{1}{n - I} \sum_{i=1}^{I} \sum_{j=1}^{n_i} (X_{ij} - X_i)^2$$

and

$$MS_{\text{between}} = \frac{1}{I - 1} \sum_{i=1}^{I} \sum_{j=1}^{n_i} (X_i - X)^2$$

are the usual mean sum of squares within and between strains, respectively, and where

$$n^* = \frac{N^2 - \sum_{i=1}^{I} n_i^2}{N(I - 1)}$$

is a correction factor for unequal strain size, which reduces to $N/I = n$ when all strains have the same number of observations, n. Note that the F-test statistic of the one-way ANOVA procedure described above equals

$$F = \frac{MS_{\text{between}}}{MS_{\text{within}}}$$

so that the estimator can be written as

$$\hat{h}^2 = \frac{F - 1}{F - 1 + 2n^*}$$

which can easily be computed from the ANOVA procedure. This estimator was used to estimate the heritability for each trait. Sometimes, a negative value of $\hat{h}^2$ occurred, which was interpreted as an estimated heritability of zero.

Note that if the strain sizes are the same for a group of traits, then the heritability scores and the P-values of the F-statistic of the ANOVA order the traits in exactly the reverse way. The strain sizes were not always exactly the same for every trait, however, but even in this case, it was found that the lower the P-value, the higher the heritability.

The null hypothesis of zero heritability was tested by a permutation test, as follows. For one trait, the total set of observations for this trait was randomly re-partitioned into I groups of sizes $n_1, \ldots, n_I$, that is, the same sizes as the original number of observations for the different mouse strains. For these new artificial strain groups, the heritability estimate was computed. This procedure was repeated 1000 times. The P-value of the test was computed as the fraction of the 1000 heritability scores that exceeded the heritability estimate of the trait. For our data, it was found that these P-values were always of the same order of magnitude as the P-values from the ANOVA. Therefore, only the latter P-values are reported, and the heritability of a trait is considered to be significant if the ANOVA of the trait indicated that there is a significant difference between mouse strains ($P < 0.005$).

Genetic correlation

To investigate the extent to which two traits share genetic factors, one may consider the correlation between the genetic effects of the two traits, or the genetic correlation. For inbred strains, the genetic correlation between two traits can be estimated as the (Pearson's linear) correlation between the eight mouse strain means of one trait and the eight mouse strain means of the other trait (Hegmann & Possidente, 1981; Crusio, 2006). The mouse strain means were taken over all slices from a given mouse strain. The estimated genetic correlations were used in a cluster analysis, as explained below.

Cluster analysis

In order to distinguish clusters of genetically correlated traits, hierarchical clustering was performed on the complete set of $n = 288$ traits. In this analysis, each trait is characterized by the eight

trait means from the eight mouse strains. To measure the distance between two traits, one minus the genetic correlation was used. Hence, traits with high genetic correlation are close to each other. Average linkage or UPGMA (Sneath & Sokal, 1973) was used as the clustering criterion. With this criterion, the distance between two clusters is the mean of the distances between all possible pairs of traits in the two clusters. A cluster analysis starts with as many clusters as there are traits, and then sequentially joins traits (or clusters of traits) that are most similar to each other to form new clusters. The result of a cluster analysis is visualized as a dendrogram, in which the sequential union of clusters is depicted together with the distance value (the position of the vertical lines along the horizontal axis) leading to this union. A dendrogram, therefore, does not define one partitioning of the dataset, but contains many different classifications. A particular classification is obtained by setting a threshold for the minimal distance that the clusters are allowed to have between them. The threshold procedure can be visualized by a horizontal line in the dendrogram; the clusters under this line are the clusters that correspond to that particular threshold.

Results

Local field potentials in hippocampal slices were measured using an eight-by-eight multi-electrode grid with 200 μm inter-electrode spacing. The electrodes were classified as lying in one of nine anatomical regions (Fig. 1B and C, and Materials and methods). The measurements were performed in mice from eight different strains, in order to estimate the heritability of amplitude and interaction measures in three experimental conditions. In the first condition, slices were perfused with ACSF, which gave rise to asynchronous activity characterized by $1/f$-like amplitude spectra (Fig. 1F). The integrated amplitudes in the frequency bands 1–4, 4–7, 7–13, 13–25, 25–35 and 35–45 Hz were computed. These amplitudes differed considerably across mouse strains (Fig. 2A). Following the ACSF condition, carbachol was applied to pharmacologically induce oscillations (see Materials and methods), which are thought to be important for hippocampal functioning during a memory-dependent task (Montgomery & Buzsáki, 2007). We observed a substantial genetic influence on the amplitude of the oscillations, as reflected by differences among the strains (Fig. 2B). Carbachol-induced oscillations depend on perisomatic inhibition (Mann *et al.*, 2005), which can be increased by the non-benzodiazepine $GABA_A$ receptor modulator zolpidem (Hájos *et al.*, 2000; Pálhalmi *et al.*, 2004). To investigate whether the role of GABAergic mechanisms are mouse strain-dependent, zolpidem was applied together with carbachol in the third condition. Also during this condition, the amplitudes were dissimilar between mouse strains (Fig. 2C), but the strain means were ordered differently than during oscillations in the absence of zolpidem. To selectively analyse the carbachol and zolpidem effect, the traits from the carbachol condition were divided by those from the ACSF condition, and the zolpidem traits were divided by the carbachol traits. In the following, the heritability and ANOVA scores of these normalized traits are discussed.

ANOVA and heritability scores

The Fourier, correlation and PLF analyses for the three conditions in the nine hippocampal subregions gave rise to a total of 288 trait values per slice (see Tables S1–S3 for lists of all traits). *P*-values from *F*-statistics (ANOVA) and heritability scores were calculated for every trait. These two measures order the traits in a reverse way (see Materials and methods). Six groups of traits are distinguished; for each condition, there is a group of traits derived with Fourier analysis

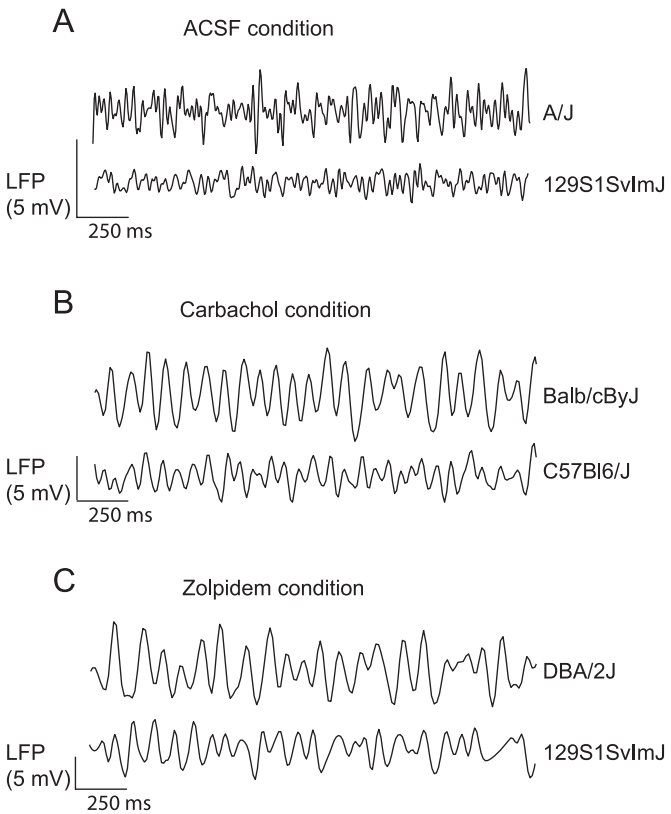

FIG. 2. Inbred mouse strains have different local field potential (LFP) amplitudes under three experimental conditions. (A) Recordings from hippocampal slices in artificial cerebrospinal fluid (ACSF) show that mouse strains differ in the amplitude of local field potential fluctuations, as illustrated by traces recorded in strains with the lowest (A/J) and highest (129S1SvImJ) amplitudes. (B) Also during carbachol-induced oscillations, the recordings showed differences in amplitudes among strains; Balb/cByJ mice had the highest amplitudes, and C57Bl6/J mice had the lowest amplitudes. (C) When zolpidem was washed in, the DBA/2J mice had the highest amplitudes, and 129S1SvImJ mice had the lowest amplitudes. The depicted signals are broadband (5–40 Hz) from the CA3 stratum pyramidale.

(containing the amplitudes in the different frequency bands from the nine anatomical regions) and one that is derived with PLF or correlation analysis (containing these measures for the 36 region pairs). Figure 3 shows, for each group, the means and error bars per mouse strain from the traits with the most significant differences between the mouse strains. For each group, the percentage of traits having an *F*-statistic with a *P*-value smaller than 0.005 was calculated; this will be referred to as *S*. In the ACSF condition, the most significant difference among the Fourier-based traits was observed for the integrated amplitude between 4 and 7 Hz in the stratum moleculare of the DG [$F_{7,97} = 7.4$, $P = 1.92 \times 10^{-6}$, $h^2 = 0.18$ (heritability), $S = 65\%$; Fig. 3A]. Among the Fourier traits in the carbachol condition, the integrated amplitude between 35 and 45 Hz in the CA1 stratum oriens was the most significant ($F_{7,84} = 5.3$, $P = 4.00 \times 10^{-5}$, $h^2 = 0.16$, $S = 36\%$; Fig. 3B). Among the Fourier traits in the zolpidem condition, the integrated amplitude between 4 and 7 Hz in the stratum moleculare of the DG varied most ($F_{7,79} = 5.7$, $P = 1.00 \times 10^{-5}$, $h^2 = 0.19$, $S = 46\%$; Fig. 3C).

Significant differences were also observed for the correlations between the nine anatomical regions in the ACSF condition and the PLF in the carbachol and zolpidem conditions. The most significant differences were the correlation between the DG stratum moleculare

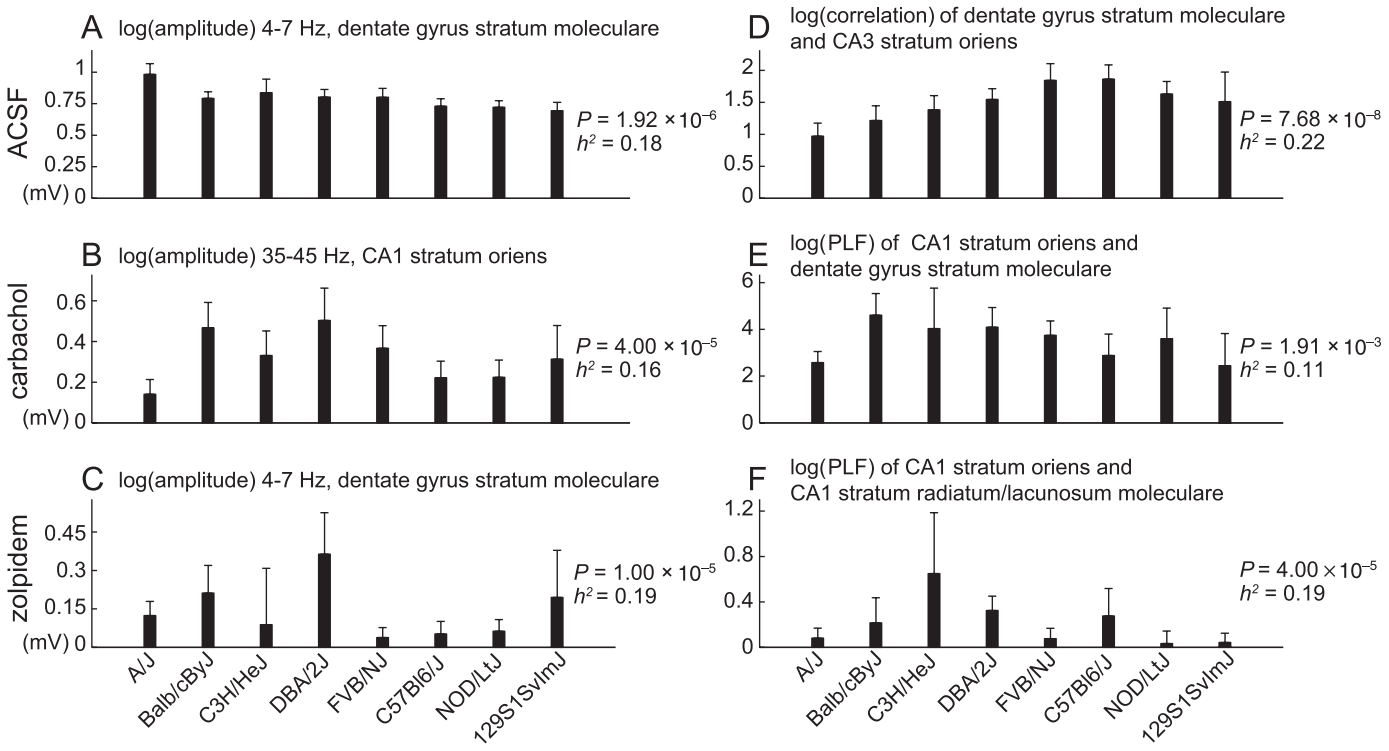

FIG. 3. The eight inbred mouse strains (horizontal axes) are ordered differently by different traits (vertical axes). Means and error bars (standard errors of the mean) of traits for the eight mouse strains. Traits with the highest heritability are shown per condition [(A and D) artificial cerebrospinal fluid (ACSF), (B and E) carbachol, and (C and F) zolpidem] and per type of measure [(A–C) amplitude, (D) inter-regional correlation, and (E and F) phase-locking factor (PLF)]. *P*-values are obtained with *F*-tests from ANOVA; h^2 = heritability. Clearly, different trait means order the mouse strains differently, suggesting that the traits depend in part on different sets of genes.

and the CA3 stratum oriens in the ACSF condition ($F_{7,98} = 8.2$, $P = 7.68 \times 10^{-8}$, $h^2 = 0.22$, $S = 47\%$; Fig. 3D), the PLF between the CA1 stratum oriens and the DG stratum moleculare in the carbachol condition ($F_{7,77} = 3.6$, $P = 1.91 \times 10^{-3}$, $h^2 = 0.11$, $S = 5\%$; Fig. 3E), and the PLF between the CA1 stratum oriens and the CA1 stratum radiatum/lacunosum moleculare in the zolpidem condition ($F_{7,70} = 5.5$, $P = 4.00 \times 10^{-5}$, $h^2 = 0.19$, $S = 7\%$; Fig. 3F). See Tables S1–S3 for the heritability scores and *P*-values for all traits.

Genetically correlated traits revealed by cluster analysis

Comparison of the traits, as illustrated in Fig. 3, reveals that the traits do not order the means of the mouse strains in the same way; that is, not all traits have a strong genetic correlation. A cluster analysis was performed to evaluate the genetic correlation structure of the complete set of 288 traits. Each trait in this analysis was characterized by eight means, one for each mouse strain. The distance measure between traits reflected genetic correlation. The number of clusters depends on the threshold for the minimal distance between the clusters (see Materials and methods). A threshold of 0.9 (allowing a maximal mean between cluster genetic correlation of 0.1) resulted in four clusters, one containing most of the traits measured in the ACSF condition, one for the carbachol condition, and two for the zolpidem condition (Fig. 4A). Besides coloring the clusters produced by the cluster analysis (Fig. 4A), we color-coded the traits according to the condition from which they were derived, in order to visualize the overlap between the three clusters and the three conditions (Fig. 4B). This clustering indicated that, in each of the three conditions, the dissimilarity between the mouse strains was of a different nature. For instance, most traits measured in the ACSF condition could not distinguish the A/J and the Balb/cByJ mice, whereas in the carbachol condition, the largest difference was between these two mouse strains. Furthermore, the C3H/HeJ mice had average mean trait values in the ACSF and carbachol conditions, whereas in the zolpidem condition they had the highest mean values of all mouse strains.

To investigate whether these four clusters could be divided into biologically relevant sub-clusters, the threshold was lowered in small steps. A threshold of 0.6 resulted in 13 clusters, which are shown in Fig. 4C. These clusters largely corresponded to three main classes of traits for each of the three conditions. For each condition, there is one class containing the interaction measures (correlations for the ACSF condition, PLFs for the carbachol and zolpidem conditions), one class containing the amplitudes in the nine regions from the low-frequency bands (1–4, 4–7 and 7–13 Hz), and one class containing the amplitudes in the high-frequency bands (13–25, 25–35 and 35–45 Hz) from each region, which suggests that low-frequency and high-frequency oscillations and interactions between areas are influenced by different genes. We color-coded the traits according to this classification (Fig. 4D), to visualize how well the clustering analysis separates these three main classes of traits within conditions. To quantify the separation, we used two measures: (i) the percentage of traits from a given class that was in the corresponding sub-cluster; and (ii) the percentage of traits in the sub-cluster that was from the given class of traits. These percentages ranged from 26 to 92% and from 35 to 93%, respectively. In particular, the correlation and PLF traits ordered the mouse strains differently from the amplitude traits; for example, in the ACSF condition, the 129S1SvImJ mice had average correlations, but rather low amplitude scores as compared with the other mouse strains.

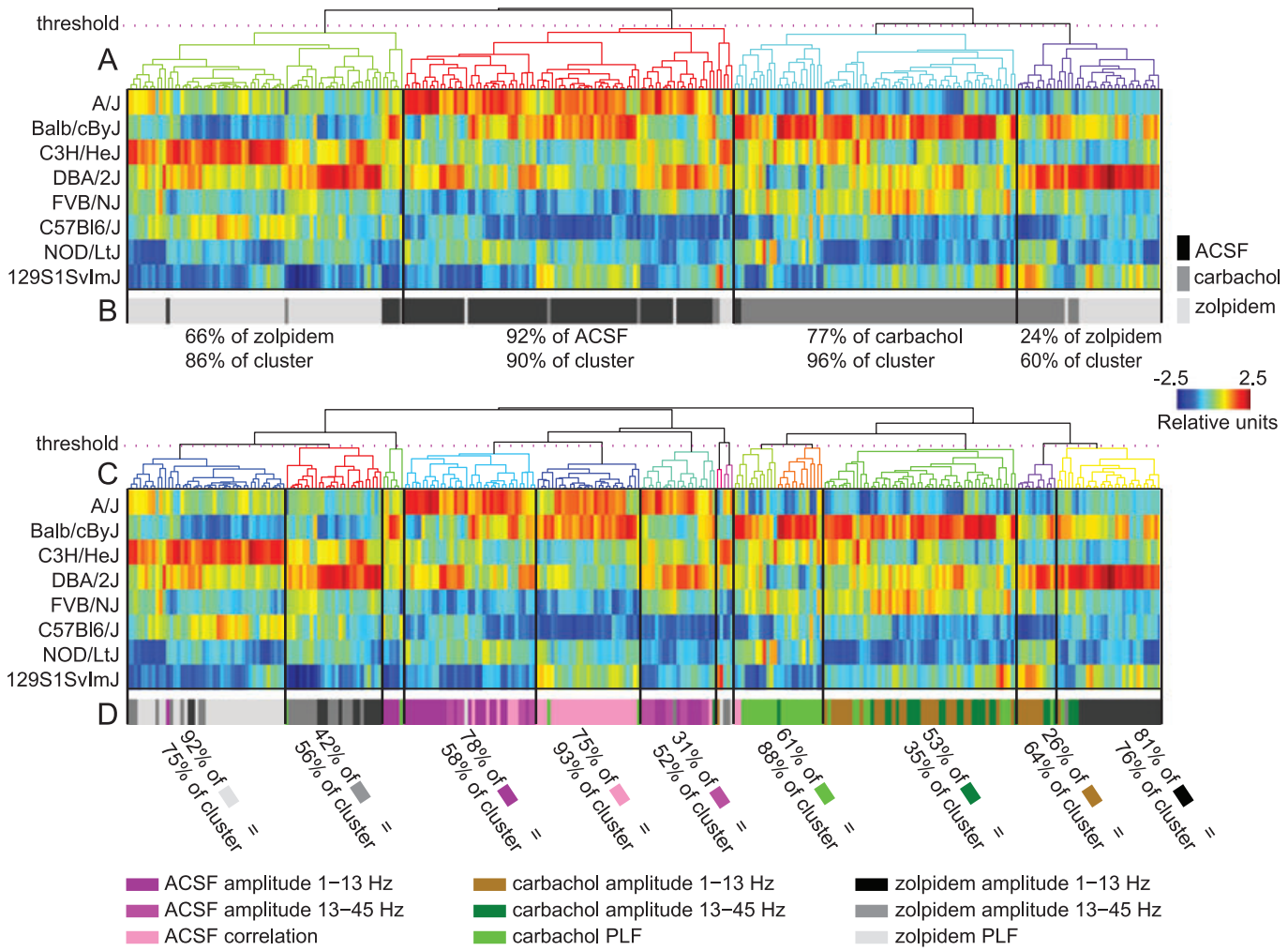

FIG. 4. Clusters of genetically correlated traits correspond to experimental conditions and types of measure. Visualizations of cluster analysis, in which each trait was characterized by its eight within-strain mean values, and traits were clustered according to their genetic correlation. (A and C) Dendrograms and corresponding color coding of the means per mouse strain for each trait, with a high (A) and a low (C) threshold. To highlight the clusters visually, every cluster has a different color in the dendrograms. Every column in the color plots corresponds to the normalized (that is, mean equals zero and variance equals one) eight strain means of a trait. The clustering in A and C suggests three and nine classes of traits, respectively. In (B) and (D) the traits are color-coded according to their classification. The percentages quantify the overlaps between classes and clusters.

In summary, selective genetic influences on brain activity were shown both in terms of a good clustering of experimental conditions and in terms of sub-clustering of main classes of quantitative traits (low and high Fourier components, and correlation).

Discussion

Variation in phenotypic traits among different mouse strains is increasingly employed to study genetic influences on physiology and behavior (Crawley *et al.*, 1997; Nguyen & Gerlai, 2002; Millstein *et al.*, 2006). We recorded ongoing activity in hippocampal slices of eight common inbred mouse strains, and found that oscillation amplitude and correlation of activity between different anatomical regions were significantly different between mouse strains and were heritable. Interestingly, the mouse strains differed in their response to the three experimental conditions, suggesting that neuronal activity in the different conditions depends in part on different sets of genes. These findings support the idea that several traits derived from hippocampal activity may be considered as endophenotypes and may be used to identify genes that code for these traits and, possibly, to unravel their contribution to behavioral or disease phenotypes.

Multiple hippocampal activity traits are heritable

The observed heritability of amplitude and correlation of activity measured in the ACSF condition could be caused by differential expression in the mouse strains of genes involved in synaptic connectivity and excitability of hippocampal neurons.

In awake animals, the power and coherence of hippocampal gamma oscillations have been shown to increase in memory tasks (Montgomery & Buzsáki, 2007). *In vitro*, these oscillations have been induced by activating three different receptors in the CA3 region: muscarinic (Mann *et al.*, 2005), metabotropic glutamate (Pálhalmi *et al.*, 2004), or kainate (Fisahn *et al.*, 2004). The oscillations induced by these methods depend mostly on the corresponding receptor families, but they all rely on inhibitory neurotransmission (Whittington *et al.*, 2000; Fisahn, 2005). This suggests that there may be some overlap in their functional roles. Here, we induced oscillations *in vitro*,

by applying the cholinergic agonist carbachol, which activates muscarinic receptors. At room temperature, these oscillations fall below the gamma range, but they share similarities with hippocampal gamma oscillations in the awake animal (Csicsvari *et al.*, 2003). We found significant heritability for oscillation amplitude as well as for correlations between areas. This may be due to strain differences in the cholinergic system (Schwegler *et al.*, 1996). Together with previous work on the involvement of hippocampal gamma oscillations in working memory tasks, our results suggest that traits derived from carbachol-induced oscillations may serve as potential endophenotypes for mnemonic functions. However, the exact role of muscarinic receptor-dependent gamma oscillations in memory remains to be investigated. Furthermore, besides the gamma generator in the CA3 region, a distinct gamma oscillator that requires input from the enthorinal cortex has been identified in the DG (Csicsvari *et al.*, 2003). Thus, although gamma oscillations *in vivo* have been implicated in memory, one should be aware that *in vitro* gamma oscillations represent only a reduced model.

We also found significant heritability in the effect of zolpidem on the amplitude and PLF of hippocampal oscillations. In a gene expression study in the striatum (Korostynski *et al.*, 2006), differences in $GABA_A$ receptor $\alpha 1$ subunits were found between two mouse strains that were also used in this study. Therefore, the differences in zolpidem responses may indicate differences in hippocampal $GABA_A$ receptor $\alpha 1$ subunit densities or localization between mouse strains. Another explanation could be that the strains may have a different interneuron morphology and/or ion channel distribution (Thomson *et al.*, 2000; Bacci *et al.*, 2003).

Interpretation of heritability and variability in neuronal activity

The heritability of a trait is a measure of the proportion of the trait's variability that is caused by genetic factors. The remainder of the variance is assumed to be caused by environmental factors. In our situation, these environmental factors do not only include those that occurred during the lifetime of the mouse. Day-to-day differences in the preparation and measurement of brain slices, for example, could also have contributed to the non-heritable variability.

The number of living cells in the hippocampal slices is another factor that may have influenced the traits. This number could, for instance, have been reduced by the stress experienced by the animal during the procedure. Given the differences between some strains in stress sensitivity (Crawley *et al.*, 1997), the number of living cells may be strain-dependent, which might have contributed to the observed between-strain differences in hippocampal activity. At present, we have no methods with which to shed light on this complex issue.

High trait heritability does not imply that the genetic basis of the trait can be found easily. On the other hand, if a trait's estimated heritability is not significantly different from zero, then there might not be any genetic influence at all, making the chances of successful gene-finding very low indeed. Moreover, if a meaningful genetic correlation between two traits is to be computed, they both need to be heritable. The heritabilities of most of the hippocampal activity traits that we derived here are significantly different from zero, which suggests that further gene-finding analysis may be successful, and this encourages the search for traits at the behavioral level with which the hippocampal traits are genetically correlated.

Cluster analysis

In the cluster analysis, the number of clusters depends on the choice of the threshold. If the threshold is lowered, the mean genetic correlation between the traits in different clusters increases. From this perspective, any threshold may reveal interesting properties of the data. We found two thresholds that resulted in biologically meaningful clusters. The higher of these two thresholds yields clusters that correspond largely to the three experimental conditions. This indicates that different genes may contribute to traits in different conditions, and that, in each condition, a partly different hippocampal mechanism could be active. The lower threshold resulted in a further subdivision of traits: per condition, there is a cluster for the high-frequency amplitude, one for the low-frequency amplitude, and one for the interaction measures of the activity. This subdivision suggests a further divergence of the genetic components of the traits according to the type of measures. This property might be reflected at the behavioral level; for example, the coherence and the amplitude of hippocampal oscillations may be related to different behavioral functions. Lower thresholds for the cluster analysis did not produce interpretable clusters. We note that there are no clusters corresponding to the nine anatomical regions. A reason for this might be that gamma oscillations are probably generated in one location, after which they spread over the rest of the hippocampus, with, as a consequence, a small inter-regional variability.

The endophenotype concept

The endophenotype strategy is one approach to decomposing a complex genetic basis into more tractable components. The hippocampus is involved in many cognitive and behavioral functions (Buzsáki, 2006). Hippocampal oscillations are network phenomena, and are influenced by many factors. Oscillation-based traits, as we have analysed here, are therefore not likely to be simple traits. We believe, however, that behavioral and cognitive traits are influenced by several complex traits in the brain, and that by looking at one of them we may reduce the complexity.

Analyses in several other directions are required in order to further investigate whether the hippocampal activity traits can be useful as endophenotypes. For example, genetic correlations between the hippocampal and behavioral traits could be computed, by using the same mouse strains for behavioral tasks (Schwegler *et al.*, 1990). Second, gene-finding analysis, for example using WebQTL (Wang *et al.*, 2003), could point to genes that underlie the traits. If feasible, genetically modified mice can then be tested to verify whether these genes are really involved in the behavioral and hippocampal traits (Nakazawa *et al.*, 2002; Bernardet & Crusio, 2006). The heritability that we have established here supports the application of these methods in further research on hippocampal activity.

Supporting Information

Additional supporting information may be found in the online version of this article:

Table S1. Heritability scores and *P*-values from *F*-statistics from the ANOVAs of all the traits derived in the artificial cerebrospinal fluid condition (spontaneous activity).

Table S2. Heritability scores and *P*-values from *F*-statistics from the ANOVAs of all the traits derived in the carbachol condition (oscillations).

Table S3. Heritability scores and *P*-values from *F*-statistics from the ANOVAs of all the traits derived in the zolpidem condition (oscillations).

Please note: As a service to our authors and readers, this journal provides supporting information supplied by the authors. Such materials are peer-reviewed and may be re-organized for online

delivery, but are not copy-edited or typeset by Wiley-Blackwell. Technical support issues arising from supporting information (other than missing files) should be addressed to the authors.

Acknowledgements

We thank Hans Lodder for expert assistance in setting up the four-fold multi-electrode array recording facility, and Cor Stoof for support in the data analysis. Part of this research was supported by a Neuro-Bsik Mouse Phenomics consortium (http://www.neurobsik.nl) grant to A. B. Brussaard. R. Jansen was supported by a Computational Life Sciences grant (635.100.005) from the Netherlands Organization for Scientific Research (NWO) to A. van Ooyen, M. de Gunst, and A. B. Brussaard. K. Linkenkaer-Hansen and H. D. Mansvelder received funding from the Innovative Research Incentive Schemes of the NWO.

Abbreviations

ACSF, artificial cerebrospinal fluid; DG, dentate gyrus; PLF, phase-locking factor.

References

Bacci, A., Rudolph, U., Huguenard, J.R. & Prince, D.A. (2003) Major differences in inhibitory synaptic transmission onto two neocortical interneuron subclasses. *J. Neurosci.*, **23**, 9664–9674.

Bernardet, M. & Crusio, W.E. (2006) Fmr1 KO mice as a possible model of autistic features. *Sci. World J.*, **6**, 1164–1176.

Buzsáki, G. (2006) *Rhythms of the Brain*. Oxford University Press, New York.

Cohen, N.J. & Eichenbaum, H. (1993) *Memory, Amnesia, and the Hippocampal System*. MIT Press, Cambridge, Massachusetts.

Crawley, J.N., Belknap, J.K., Collins, A., Crabbe, J.C., Frankel, W., Henderson, N., Hitzemann, R.J., Maxson, S.C., Miner, L.L. & Silva, A.J. (1997) Behavioral phenotypes of inbred mouse strains: implications and recommendations for molecular studies. *Psychopharmacology*, **132**, 107–124.

Crusio, W. (2006) *An introduction of quantitative genetics*. In Jones, B.C. & Mormède, P. (eds), *Neurobehavioral Genetics: Methods and Applications*. CRC Press, Boca, chapter 4.

Csicsvari, J., Jamieson, B., Wise, K.D. & Buzsáki, G. (2003) Mechanisms of gamma oscillations in the hippocampus of the behaving rat. *Neuron*, **37**, 311–322.

Fernandes, C., Paya-Cano, J.L., Sluyter, F., D'Souza, U., Plomin, R. & Schalkwyk, L.C. (2004) Hippocampal gene expression profiling across eight mouse inbred strains: towards understanding the molecular basis for behaviour. *Eur. J. Neurosci.*, **19**, 2576–2582.

Fisahn, A. (2005) Kainate receptors and rhythmic activity in neuronal networks: hippocampal gamma oscillations as a tool. *J. Physiol.*, **562**, 65–72.

Fisahn, A., Pike, F.G., Buhl, E.H. & Paulsen, O. (1998) Cholinergic induction of network oscillations at 40 Hz in the hippocampus *in vitro*. *Nature*, **394**, 186–189.

Fisahn, A., Contractor, A., Traub, R.D., Buhl, E.H., Heinemann, S.F. & McBain, C.J. (2004) Distinct roles for the kainate receptor subunits GluR5 and GluR6 in kainate-induced hippocampal gamma oscillations. *J. Neurosci.*, **24**, 9658–9668.

Flint, J. & Munafo, M.R. (2007) The endophenotype concept in psychiatric genetics. *Psychol. Med.*, **37**, 163–180.

de Geus, E.J.C. (2002) Introducing genetic psychophysiology. *Biol. Psychol.*, **61**, 1–10.

Gottesman, I.I. & Gould, T.D. (2003) The endophenotype concept in psychiatry: etymology and strategic intentions. *Am. J. Psychiatry*, **160**, 636–645.

Hájos, N., Nusser, Z., Rancz, E.A., Freund, T.F. & Mody, I. (2000) Cell type- and synapse-specific variability in synaptic $GABA_A$ receptor occupancy. *Eur. J. Neurosci.*, **12**, 810–818.

Hegmann, J.P. & Possidente, B. (1981) Estimating genetic correlations from inbred strains. *Behav. Genet.*, **11**, 103–114.

Hovatta, I., Tennant, R.S., Helton, R., Marr, R.A., Singer, O., Redwine, J.M., Ellison, J.A., Schadt, E.E., Verma, I.M., Lockhart, D.J. & Barlow, C. (2005) Glyoxalase 1 and glutathione reductase 1 regulate anxiety in mice. *Nature*, **438**, 662–666.

Korostynski, M., Kaminska-Chowaniec, D., Piechota, M. & Przewlocki, R. (2006) Gene expression profiling in the striatum of inbred mouse strains with distinct opioid-related phenotypes. *BMC Genomics*, **7**, 146.

Lachaux, J.P., Rodriguez, E., Martinerie, J. & Varela, F.J. (1999) Measuring phase synchrony in brain signals. *Hum. Brain Mapp.*, **8**, 194–208.

Mann, E.O., Suckling, J.M., Hájos, N., Greenfield, S.A. & Paulsen, O. (2005) Perisomatic feedback inhibition underlies cholinergically induced fast network oscillations in the rat hippocampus *in vitro*. *Neuron*, **45**, 105–117.

Millstein, R.A., Ralph, R.J., Yang, R.J. & Holmes, A. (2006) Effects of repeated maternal separation on prepulse inhibition of startle across inbred mouse strains. *Genes Brain Behav.*, **5**, 346–354.

Mitzdorf, U. (1985) Current source-density method and application in cat cerebral cortex: investigation of evoked potentials and EEG phenomena. *Physiol. Rev.*, **65**, 37–100.

Montgomery, S.M. & Buzsáki, G. (2007) Gamma oscillations dynamically couple hippocampal CA3 and CA1 regions during memory task performance. *Proc. Natl Acad. Sci. USA*, **104**, 14495–14500.

Nakazawa, K., Quirk, M.C., Chitwood, R.A., Watanabe, M., Yeckel, M.F., Sun, L.D., Kato, A., Carr, C.A., Johnston, D., Wilson, M.A. & Tonegawa, S. (2002) Requirement for hippocampal CA3 NMDA receptors in associative memory recall. *Science*, **297**, 211–218.

Nguyen, P.V. & Gerlai, R. (2002) Behavioural and physiological characterization of inbred mouse strains: prospects for elucidating the molecular mechanisms of mammalian learning and memory. *Genes Brain Behav.*, **1**, 72–81.

Pálhalmi, J., Paulsen, O., Freund, T.F. & Hájos, N. (2004) Distinct properties of carbachol- and DHPG-induced network oscillations in hippocampal slices. *Neuropharmacology*, **47**, 381–389.

Plomin, R. & Crabbe, J. (2000) DNA. *Psychol. Bull.*, **126**, 806–828.

Schwegler, H., Crusio, W.E., Brust, I. & Specificity, S. (1990) Hippocampal mossy fibers and radial-maze learning in the mouse: a correlation with spatial working memory but not with non-spatial reference memory. *Neuroscience*, **34**, 293–298.

Schwegler, H., Boldyreva, M., Pyrlik-Göhlmann, M., Linke, R., Wu, J. & Zilles, K. (1996) Genetic variation in the morphology of the septo-hippocampal cholinergic and GABAergic system in mice. I. Cholinergic and GABAergic markers. *Hippocampus*, **6**, 535–545.

Shute, C.C.D. & Lewis, P.R. (1963) Cholinesterase-containing systems of the brain of the rat. *Nature*, **199**, 1160–1164.

Sneath, P.H.A. & Sokal, R.R. (1973) *Numerical Taxonomy.* Freeman, San Francisco.

Squire, L.R. & Butters, N. (2002) *Neuropsychology of Memory.* Guilford Press, New York.

Tass, P., Rosenblum, M.G., Weule, J., Kurths, J., Pikovsky, A., Volkmann, J., Schnitzler, A. & Freund, H.J. (1998) Detection of n: m phase locking from noisy data: application to magnetoencephalography. *Phys. Rev. Lett.*, **81**, 3291–3294.

Thomson, A.M., Bannister, A.P., Hughes, D.I. & Pawelzik, H. (2000) Differential sensitivity to zolpidem of IPSPs activated by morphologically identified CA1 interneurons in slices of rat hippocampus. *Eur. J. Neurosci.*, **12**, 425–436.

Wang, J., Williams, R.W. & Manly, K.F. (2003) WebQTL. *Neuroinformatics*, **1**, 299–308.

Welch, P. (1967) The use of fast Fourier transform for the estimation of power spectra: a method based on time averaging over short, modified periodograms. *IEEE Trans. Audio Electroacoustics*, **15**, 70–73.

Whittington, M.A., Traub, R.D., Kopell, N., Ermentrout, B. & Buhl, E.H. (2000) Inhibition-based rhythms: experimental and mathematical observations on network dynamics. *Int. J. Psychophysiol.*, **38**, 315–336.